ACS OMEGA

http://pubs.acs.org/journal/acsodf

Article

Exploration of Photophysical and Nonlinear Properties of Salicylaldehyde-Based Functionalized Materials: A Facile Synthetic and DFT Approach

Muhammad Imran, Muhammad Khalid,* Rifat Jawaria, Asif Ali, Muhammad Adnan Asghar, Zahid Shafiq, Mohammed A. Assiri, Hafiza Munazza Lodhi, and Ataualpa Albert Carmo Braga

Cite This: *ACS Omega* 2021, 6, 33914−33922

Read Online

ACCESS | Metrics & More | Article Recommendations | Supporting Information

ABSTRACT: The current research presents the synthesis of novel salicylaldehyde thiosemicarbazones (**1**−**6**) and their spectroscopic characterization employing UV−visible, Fourier transform infrared spectroscopy, and NMR techniques. Experimental results are compared and validated with the results obtained theoretically by employing density functional theory at the M06 level with the 6-311G (d,p) basis set. Further, various parameters [natural bond orbital (NBO)], linear and nonlinear optical (NLO) properties, and global reactivity parameters (GRPs) are computationally calculated. The NBO approach has confirmed the stability of compounds on account of charge delocalization and hyper conjugative interaction network. Frontier molecular orbital analysis has explained the charge transfer and chemical reactivity capability, while GRPs have led to the analysis of kinetic stability of the studied molecules. Further, the probability of being NLO-active has been theoretically proved by the HOMO/LUMO energy difference (4.133−4.186 eV) and β values (192.778−501.709 a.u). These findings suggest that the studied compounds possess potential NLO applications as they have shown larger NLO values in comparison with that of the urea molecule, and such distinct properties prove their technological importance.

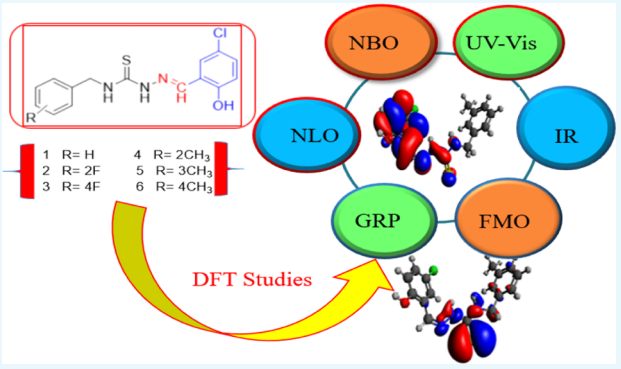

1. INTRODUCTION

Salicylaldehyde and its derivatives are important organic synthetic precursors and chelating agents.[1] Thiosemicarbazones (TSCs) can generally be synthesized from the reaction of a thiosemicarbazide with aldehydes or ketones and are versatile Schiff base ligands consisting of an azomethine linkage group (−CH═N−).[2] TSC derivatives show a broad range of biological properties and are being utilized for the treatment of many diseases. The biological properties of TSCs frequently manifested a high reliance on their substituents. Their anticancer,[3] anti-inflammatory,[4] antihypertensive,[5] antibacterial,[6] antitumor,[7] antimalarial,[8] antiamoebic,[9] antiviral,[10] antitubercular,[11] antifungal,[12] trypanocidal,[13] anticonvulsant,[14] anti-HIV,[15] local anesthetic,[16] hypoglycemic,[17] and cytotoxic activities[18,19] are generally accepted. TSCs also play an important role in analytical chemistry, inorganic chemistry, organic synthesis, oxidation catalysis,[20] electrochemistry,[21] metal refining, photography, and electroplating.[22] Nonlinear optical (NLO) properties and density functional theory (DFT) are the research disciplines in which the TSC derivatives are determined by theoretical as well as experimental methods. DFT and TD-DFT (time-dependent density functional theory) approaches have provided auspicious vision concerning the chemical and biological systems.[23] The structural parameters like molecular geometry and vibrational frequencies can be determined by employing DFT calculations.[24] NLO materials are versatile and can be used in the telecommunication sector due to intramolecular charge transfer (ICT) and their ability to delocalize the electrons. The optoelectronic technologies have opened the doors of research toward outstanding NLO materials.[25] NLO materials exhibit several applications like electro-optic variations, photonics, and better optical signal processing and also find a valuable role in technologies of optical communication.[26] The concepts of polarizability and hyperpolarizability are useful[27] for explaining the structure−property of molecules concerning their NLO characters.[28]

Received: September 19, 2021
Accepted: November 23, 2021
Published: December 3, 2021

https://doi.org/10.1021/acsomega.1c04984
ACS Omega 2021, 6, 33914−33922

Scheme 1. Synthetic Route of TSCs 1−6

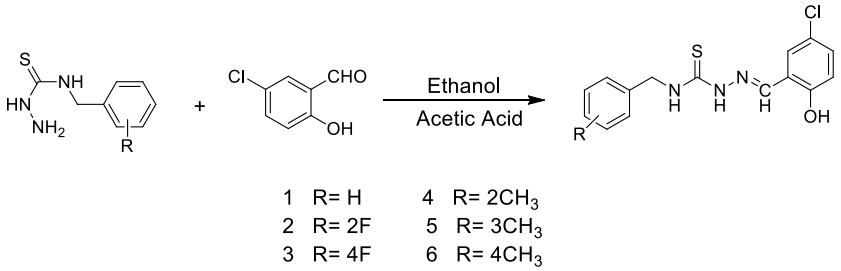

We report herein the synthesis and spectroscopic and computational studies of novel TSCs (**1−6**) and the comparative analysis of experimental and theoretical work via DFT and computational modeling to investigate the properties of six novel salicylaldehyde-based TSCs, which yields significant aspects according to the theme of research work.

2. COMPUTATIONAL STUDIES

Gaussian 09 program package[29] using M06 functional[30] with the 6-311G (d,p) basis set (a split-valence triple-zeta basis plus d, p polarization functions on non-hydrogen and hydrogen, respectively)[31] was operated to execute quantum chemical computations for investigated compounds with the support of a package to determine the vibrational wave numbers and NLO and natural bond orbital (NBO) properties. Avogadro,[32] GaussSum,[33] GaussView 5.0,[34] and Chemcraft[35] programs were used to create input files as well as for the elucidation of output files. Furthermore, for frontier molecular orbital (FMO) and UV−visible analyses, TD-DFT[36,37] calculations were performed at the mentioned level and basis set. M06/6-311G (d,p) is a hybrid technique. It is a highly parameterized approximate exchange−correlation energy functional in DFT.[38,40] To examine the global reactivity parameters (GRPs) such as reactivity, energy, and stability of compounds, the HOMO−LUMO energy gaps were used.[39]

3. RESULTS AND DISCUSSION

The derivatives of salicylaldehyde-based TSCs were synthesized according to Scheme 1 in high yield. IR and NMR techniques were utilized to identify the structures of the synthesized compounds. The IR spectra of entitled compounds displayed absorption bands in the functional group region. The characteristic absorption band at 1217−1229 cm^{-1} was responsible for the C═S vibration in compounds (**1−6**). Moreover, the disappearance of the C═O peak at 1680 cm^{-1} and the appearance of a new absorption peak at 1539−1548 cm^{-1} which belongs to C═N moiety confirmed the formation of Schiff base in compounds (**1−6**). The intense peak appearing at 2996−3218 cm^{-1} corresponded to the N−H group in compounds (**1−6**).

The ^{1}H NMR spectra of compounds (**1−6**) displayed signals for both aromatic and aliphatic protons. The doublet peak at 4.751−4.855 ppm is attributed to CH_2N protons in compounds (**1−6**). The signal for compounds (**1−6**) at 9.094−9.155 ppm corresponded to the CH_2−NH proton as expected. Furthermore, the hydrazinic (NHN) proton displayed a deshielded singlet signal at 11.544−11.663 in compounds (**1−6**). The signal for the hydroxyl (OH) proton appeared at the slightly deshielded region at 8.300−8.331 ppm. The singlet peak was observed for the CH═N proton at 10.236−10.277 ppm for compounds (**1−6**). The signal for methyl (CH_3) protons in compounds 4, 5, and 6 aroused at 2.257, 2.232, and 2.257 ppm, respectively. All aromatic protons displayed a multiplet signal in the range of 6.783−8.160 ppm for compounds (**1−6**).

3.1. NBO Analysis. NBO analysis is a helpful tool for the investigation of transfer of charges between vacant and filled orbitals,[41] interactions between bonds, interpretation of hyper conjugative interactions, and distribution of charges. This analysis is also used to observe the transference of charge densities from the donor to the acceptor in donor π-acceptor configurations.[42] These calculations are often adapted to disclose about the atomic charge, orbital interactions, and orbital hybridization.[43] This is also an appealing technique for chemists for explaining the inter and intramolecular transition results ascertained by virtual and filled orbitals.[44] The main reason to yield remarkable stabilization energies are the interactions of donors and acceptors.[45]

The NBO analysis is performed by applying the M06/6-311G(d,p) level of theory as described in Tables S1−S6. The formula of stabilization energy relevant to the second-order perturbation technique is presented by eq 1.

$$E^{(2)} = q_i \frac{(F_{i,j})^2}{\varepsilon_j - \varepsilon_i} \quad (1)$$

where $E^{(2)}$ denotes the stabilization energy, q_i refers to the donor-orbital occupancy, $F(i,j)$ indicates the off-diagonal NBO Fock matrix elements, and ε_i and ε_j point out the diagonal elements.

Usually, four types of electronic transitions $\sigma \rightarrow \sigma^*$, $\pi \rightarrow \pi^*$, LP $\rightarrow \sigma^*$, and LP $\rightarrow \pi^*$ were identified for entitled products. Among these $\pi \rightarrow \pi^*$ transitions were noticed as the most prominent transitions having a higher value of stabilization energy, while LP $\rightarrow \pi^*$ and LP $\rightarrow \sigma^*$ transitions were less dominant. In contrast, $\sigma \rightarrow \sigma^*$ transitions were the least dominant with smaller magnitudes of values. The presence of charge transfer and conjugation in compounds (**1−6**) can be inspected by studying the $\pi \rightarrow \pi^*$ transitions. The most significant $\pi \rightarrow \pi^*$ transitions were π(C25−C27) $\rightarrow \pi^*$(C28−C30), π(C24−C26) $\rightarrow \pi^*$(C27−C29), π(C22−C24) $\rightarrow \pi^*$(C25−C27), π(C3−C4) $\rightarrow \pi^*$(C1−C2), π(C22−C24) $\rightarrow \pi^*$(C25−C27), and π(C24−C26) $\rightarrow \pi^*$(C27−C29) with the highest value of stabilization energies 26.43, 26.37, 26.47, 23.80, 26.43, and 26.42 kcal/mol found in compounds (**1−6**), respectively. Moreover, other $\pi \rightarrow \pi^*$ transitions like π(C17−S18) $\rightarrow \pi^*$(C17−S18), π(C4−C5) $\rightarrow \pi^*$(C4−C5), π(C14−S15) $\rightarrow \pi^*$(C14−S15), π(N19−C20) $\rightarrow \pi^*$(N19−C20), π(N18−C19) $\rightarrow \pi^*$(N18−C19), and π(N20−C21) $\rightarrow \pi^*$(N20−C21) yield least stabilization energies values of 0.57, 0.51, 0.75, 1.01, 1.12, and 1.13 kcal/mol for compounds (**1−6**), respectively (Tables S1−S6).

https://doi.org/10.1021/acsomega.1c04984
ACS Omega 2021, 6, 33914−33922

The greater values for $\sigma \rightarrow \sigma^*$ transitions were observed at 9.09, 9.09, 9.06, 8.85, 7.39, and 9.08 for σ(C22−H23) → σ^*(N19−N21), σ(C21−H22) → σ^*(N18−N20), σ(C19−H20) → σ^*(N16−N18), σ(C20−H21) → σ^*(N1−N19), σ(C14−S15) → σ^*(C14−S15), and σ(C21−H22) → σ^*(N18−N20) in compounds (**1**−**6**), respectively. In the same scenario, some other transitions σ(C17−C19) → σ^*(N19−H20), σ(C13−C11) → σ^*(C11−H13), σ(C27−H29) → σ^*(C24−H28), σ(C20−C22) → σ^*(C20−H21), σ(C1−H34) → σ^*(C1−C2), and σ(C1−H7) → σ^*(C2−H8) observed in compounds (**1**−**6**) and the stabilization energy values are noticed to be 0.52, 0.54, 0.80, 0.58, 0.69, and 0.76 kcal/mol, respectively (Tables S1−S6). These least stabilization energy values were examined owing to the occurrence of feeble interactions among electron donor−acceptor moieties.

Furthermore, significant transitions from LP → σ^* and LP → π^* were also seen in case of resonance, such as LP1(N15) → σ^*(C17−S18), LP1(N14) → σ^*(C16−S17), LP1(N12) → σ^*(C14−S15), LP1(N13) → σ^*(C15−S16), LP1(N12) → σ^*(C14−S15), and LP1(N14) → σ^*(C16−S17) with large values of stabilization energy 51.48, 57.49, 48.81, 69.80, 54.13, and 4.80 kcal/mol in compounds (**1**−**6**), respectively. For compounds (**1**−**6**), other resonance interactions with the least value of stabilization energies 0.52, 0.61, 0.65, 0.53, 0.52, and 0.52 were observed for LP2(Cl35) → σ^*(C24−C26), LP1(N14) → π^*(C16−S17), LP1(N12) → σ^*(C3−C9), LP2(S16) → σ^*(C3−C10), LP2(Cl32) → σ^*(C21−C23), and LP1(N14) → σ^*(C3−C11), respectively (Tables S1−S6). Hence, based on the NBO analysis, it can be determined that hyperconjugative interactions, intermolecular charge transfer, and extended conjugation play a momentous role in providing stability to the entitled compounds and verifies charge-transfer characteristics which are essential for potent NLO properties. Some transitions closely resemble with our previous article.

3.2. UV−Visible Analysis. Ultraviolet−visible (UV−vis) spectroscopy presents a valuable understanding concerning the probability of charge transfer, nature of electronic transitions, and contributing configurations to the transitions. TD-DFT at the M06/6-311G (d,p) level of theory was employed to execute the UV−visible absorption spectra. The absorption peak (λ_{max}), vertical excitation energies, oscillator strength (f), and transition assignments of the investigated compounds are given in Table S7. The tabularized outcome illustrates that the fundamental absorption maxima of compounds (**1**−**3**) appeared in the range of 272−390, 277−388, and 275−388 nm which was in good agreement with the experimentally reported λ_{max} values: 241, 240, and 220, respectively. Furthermore, the experimental λ_{max} values 219, 296, and 245 nm, respectively, for compounds (**4**−**6**) matched nicely with the DFT absorption bands 275−389, 273−391, and 273−392 nm, respectively. Overall, the experimentally calculated λ_{max} showed appropriate harmony with the DFT calculated λ_{max} of compounds (**1**−**6**) as expressed in Table S7.

3.3. Vibrational Analysis. The IR spectral data of the synthesized compounds exhibited significant absorptions in the functional group region. The absorption frequencies are listed in the Supporting Information (Tables S8−S13). The scaling factors, 0.958 for the calculated frequencies in the range from 4000 to 1700 cm^{-1} and 0.983 for frequencies lower than 1700 cm^{-1}, were used.[46]

3.3.1. C−H Vibrations. C−H vibrational bands are commonly noticed due to stretching and bending vibrational modes. C−H vibrational bands in aromatic and heteroaromatic rings, on account of stretching mode, emerged at 3100−3000 cm^{-1}.[47] Mixed DFT computed stretching frequencies in compounds (**1**−**6**) were calculated at 3170, 3179, 3163, 3163, 3177, and 3149 cm^{-1} that are robustly supported by experimental data at 3153, 3187, 3125, 3134, 3218, and 3130 cm^{-1}. In compounds (**1**−**6**), the DFT-calculated bending vibrations were found at 1361, 1360, 1377, 1323, 1314, and 1357 cm^{-1} which was in correlation with the experimental bending modes (Tables S8−S13).

3.3.2. C═N Vibrations. Experimental C═N stretching vibrations in entitled compounds were in the range of 1548, 1532, 1548, 1541, 1543, and 1539 cm^{-1}, while DFT-scaled vibrations are found in good agreement at 1621, 1522, 1620, 1524, 1520, and 1621 cm^{-1}, respectively (Tables S8−S13).

3.3.3. N−H Vibrations. Generally, the N−H vibrations lie in the range of 3450−3250 cm^{-1}.[48] DFT-scaled computed stretching vibrational bands at 3315, 3318, 3311, 3030, 3313, and 3311 cm^{-1} were detected to be associated with N−H, which agree with the experimentally calculated results at 3148, 3323, 3450, 3134, 3342, and 3282 cm^{-1}, respectively, for compounds (**1**−**6**). Moreover, the theoretically observed N−H bending vibrational modes were measured at 1488, 1490, 1491, 1496, 1520, and 1492 cm^{-1} which express excellent correspondence with the experimentally measured bands 1523, 1532, 1511, 1522, 1543, and 1514 cm^{-1}, respectively (Tables S8−S13).

3.3.4. C−C Stretching Vibrations. Usually, the C−C stretching frequencies in the benzene ring lie in the region of 1650−1400 cm^{-1}.[49] In compounds (**1**−**6**), the computed vibrational bands in the benzene ring at 1492, 1500, 1518, 1524, 1488, and 1508 cm^{-1} show consistency with the literature. Moreover, DFT-scaled vibrational data associated satisfactorily with the experimental vibrational data measured at 1548, 1532, 1530, 1541, 1538, and 1532 cm^{-1} for compounds (**1**−**6**), respectively (Tables S8−S13).

3.3.5. C═S Vibrations. The C═S vibrational frequencies appear at 1500−1200 cm^{-1}. DFT-scaled computed vibrational bands of C═S were noticed at 1226, 1210, 1219, 1219, 1220, and 1217 cm^{-1} which are in accordance with experimental frequencies 1229, 1222, 1217, 1228, 1223, and 1225 cm^{-1} for compounds (**1**−**6**), respectively (Tables S8−S13).

3.3.6. O−H Vibrations. The O−H vibration is a remarkable stretching vibration that generally appears at 3700−3550 cm^{-1}.[50] In the investigated compounds (**1**−**6**), the O−H scaled stretching modes are observed at 3723, 3724, 3726, 3724, 3725, and 3727 cm^{-1} which display excellent concurrence with the experimentally determined values 3687, 3687, 3656, 3386, 3687, and 3719 cm^{-1}, respectively (Tables S8−S13).

3.3.7. C-X Vibrations. The C−Cl stretching vibrational peaks normally seem at 800 cm^{-1}.[51] The DFT-scaled calculated C−Cl vibrational bands for compounds (**1**−**6**) are noticed at 851, 908, 849, 853, 849, and 846 cm^{-1}, respectively, which reflect consistency with the experimentally measured stretching bands. In compounds 2 and 3, C−F theoretical vibrations were noted at 805 and 845 cm^{-1}, respectively.

From the previous argument, it is manifested that the experimental Fourier transform infrared spectroscopy outcomes show good resemblance with the resultant computed simulated ones as provided in Tables S8−S13.

3.4. FMO. FMO investigation assists to elucidate the optical properties and chemical stability of molecules.[52] Energies and energy gap of HOMO−LUMO describe the several

https://doi.org/10.1021/acsomega.1c04984
ACS Omega 2021, 6, 33914−33922

Table 1. FMO Energies of Compounds 1−6[a]

	1		2		3		4		5		6	
$MO_{(S)}$	E (eV)	ΔE	E (eV)	ΔE	E (eV)	ΔE	E (eV)	ΔE	E (eV)	ΔE	E (eV)	ΔE
HOMO	−5.762	4.162	−5.748	4.179	−5.837	4.186	−5.784	4.151	−5.743	4.146	−5.719	4.133
LUMO	−1.600		−1.569		−1.651		−1.633		−1.597		−1.586	

[a]E = energy, $\Delta E = E_{LUMO} - E_{HOMO}$, MO(s) = molecular orbitals, HOMO = highest occupied molecular orbital, and LUMO = lowest unoccupied molecular orbital.

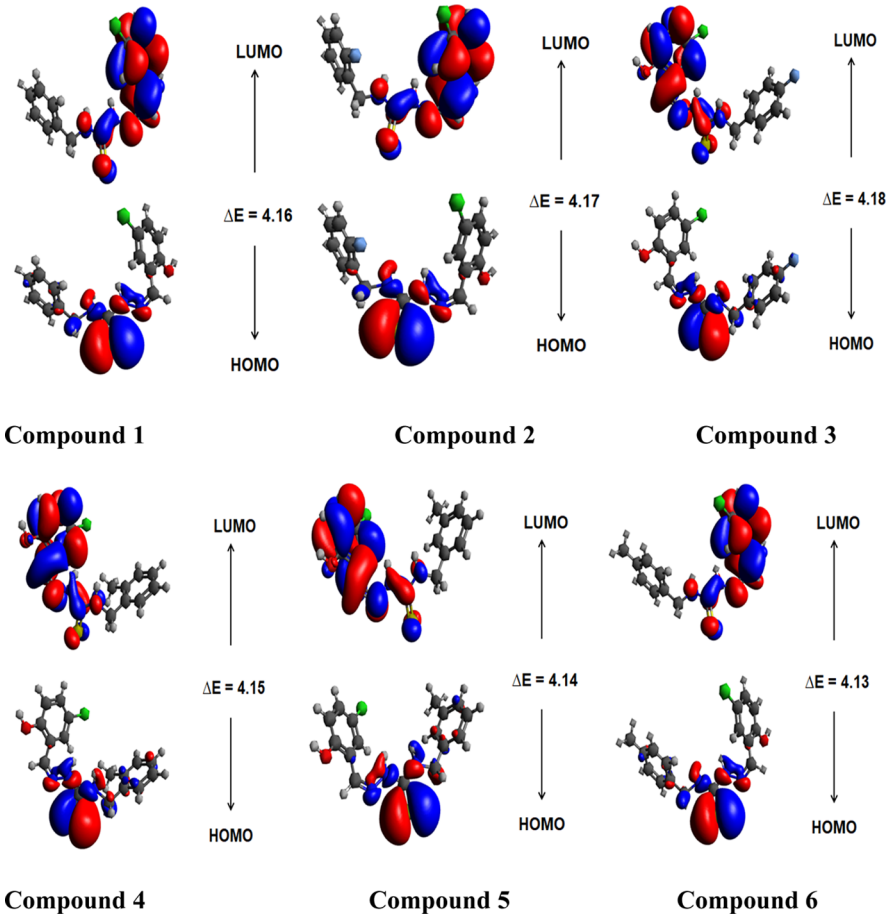

Figure 1. FMOs of the title compounds.

approaches which include optical and electronic properties, charge transfer, UV−vis spectra, chemical hardness, softness, reactivity, and numerous interactions between molecules.[53,54] The large value of the HOMO−LUMO energy gap (E_{gap}) revealed the compound to be harder having low chemical reactivity and high kinetic strength and vice versa.[55] More polarized molecules are illustrated to bear NLO properties.[56]

The energy calculations were executed by the use of DFT/M06/6-311G (d,p) basis sets. The energies and pictorial description of HOMO, LUMO, HOMO-1 and LUMO+1, and HOMO-2 and LUMO+2 (Figure S1) for investigated compounds are shown in (Tables 1 and S14).

The energy gaps of compounds (**1**−**6**) are computed to be 4.162, 4.179, 4.186, 4.151, 4.146, and 4.133 eV, respectively. The energy gap in the decreasing order of studied compounds is found to be **3** > **2** > **1** > **4** > **5** > **6**. Moreover, the energy difference between HOMO-1 and LUMO+1 is obtained as 5.523, 5.495, 5.533, 5.468, 5.498, and 5.499 eV for all studied compounds (**1**−**6**), and the HOMO-2 and LUMO+2 energy gap of orbitals is noticed to be 6.366, 6.13, 6.192, 6.454, 6.399, and 6.4 eV, respectively. The highest value of the energy gap investigated is for compound **3** (4.186 eV), while the lowest value determined is for compound **6** (4.133 eV) that signifies proficient ICT communication. In HOMO, the charge density is located on the 4-methyl-1-methylenethiosemicarbazide part, while in LUMO, the concentration of charge density is on (E)-1-(5-chloro-2-hydroxybenzylidene) thiosemicarbazide for compounds (**1**−**6**), as represented in Figure 1.

3.5. GRPs. HOMO and LUMO energies can be employed to illustrate the stability performance of compounds[1−6] in terms of GRP descriptors.[57−59] The value of the energy gap ($\Delta E = E_{(LUMO)} - E_{(HOMO)}$) is in inverse relation to the softness and reactivity of the species under study and in direct relation with the hardness and stability of the compounds. Subsequently, molecules that possess a larger value of energy gap (ΔE) are considered as hard compounds which resist change in electronic configurations and therefore have a greater kinetic strength and least reactivity. While on the other hand, the molecules which possess a less energy gap value are regarded as soft molecules having easily tunable character, less stability,

https://doi.org/10.1021/acsomega.1c04984
ACS Omega 2021, 6, 33914−33922

Table 2. GRPs of Compounds (1−6)[a]

compounds	I	E	X	η	μ	ω	σ
1	5.762	1.6	3.681	2.081	−3.681	3.255589	0.240269
2	5.748	1.569	3.6585	2.0895	−3.6585	3.202829	0.239292
3	5.837	1.651	3.744	2.093	−3.744	3.348671	0.238892
4	5.784	1.633	3.7085	2.0755	−3.7085	3.313171	0.240906
5	5.743	1.597	3.67	2.073	−3.67	3.248649	0.241196
6	5.719	1.586	3.6525	2.0665	−3.6525	3.227863	0.241955

[a]Ionization potential (I), electron affinity (E), electronegativity (X), global hardness (η), chemical potential (μ), global electrophilicity (ω), and global softness (σ).

and high reactivity. The studied compounds (**1**−**6**) showed greater values of ionization potential in comparison to electron affinity as demonstrated in Table 2. The values of ionization potential and electron affinity for compounds **1**, **3**, **4**, and **6** are found to be greater than those for compounds **2** and **5**. The observed chemical hardness values for compounds (**1**−**6**) are greater as compared to softness values. By comparing compounds (**1**−**6**), it was observed that compound **3** has greater hardness and the lowest softness value. This depicts that compound **3** is hard, least reactive, and most stable than **1**, **2**, **4**, **5**, and **6** (Table 2). Chemical potential which provides support to explain the stability and reactivity of compounds (**1**−**6**) is in direct association with the stability and in inverse relation to the reactivity of the compounds under examination. The order of chemical potential in compounds (**1**−**6**) is as follows

$$[6(\mu = -3.6525\ \text{eV})] < [2\ (\mu = -3.6585\ \text{eV})] < [5\ (\mu = -3.67\ \text{eV})] < [1\ (\mu = -3.681\ \text{eV})] < [4\ (\mu = -3.7085\ \text{eV})] < [3\ (\mu = -3.744\ \text{eV})]$$

This parameter also revealed that compound **3** having the greater chemical potential value is the more stable and the least reactive compound, whereas compound **6** is the less stable and the highly reactive compound among compounds (**1**−**6**). From earlier debate, it is manifested that the entire studied compounds are chemically stable and hard molecules.

3.6. NLO Properties. Over the past few years, the finding of compounds having characteristic NLO properties is receiving notable attention owing to their advantages in optoelectronic technologies and the telecommunication area. Computational and experimental communities of physics, chemistry, and material sciences are presenting multidisciplinary attempts in the improvement of NLO materials owing to its value in providing the crucial functions of enhanced optical signal processing, frequency mixing, electro-optic modulation for data storage, higher data rates, and harmonic generation in optical communication technologies.[60−62] For explaining the structure−property of a molecule concerning the NLO characters, the concepts of polarizability and hyperpolarizability are helpful.[63] In addition to the NLO response, the properties of organic compounds offer a crucial role in the internal charge-transfer process and extended π-conjugated systems.[64]

The linear optical response (polarizability) and NLO response including first hyperpolarizability (β_{tot}) are determined by employing the M06/6-311G(d,p) functional. The polarizability $<\alpha>$ and hyperpolarizability (β) values are calculated by the following equations: Polarizability $<\alpha>$ equation along x-, y-, and z-axes[65]

$$<\alpha> = 1/3(\alpha_{xx} + \alpha_{yy} + \alpha_{zz}) \quad (2)$$

Hyperpolarizability (β) equation along x-, y-, and z-axes

$$\beta_{tot} = [(\beta_{xxx} + \beta_{xyy} + \beta_{xzz})^2 + (\beta_{yyy} + \beta_{yzz} + \beta_{yxx})^2 + (\beta_{zzz} + \beta_{zxx} + \beta_{zyy})^2]^{1/2} \quad (3)$$

The calculated results are presented in Tables S15 & S16. The total value of dipole moment, the average polarizability along x-, y-, and z-directions, and the hyperpolarizability value along with its tensors are presented in Tables S15−S17. The average dipole moment was found to be 7.4458, 7.9529, 6.8301, 7.5562, 7.6516, and 7.6528 D, respectively, for all studied compounds. Results revealed the highest dipole moment value for compound **2** at 7.9529 D, while the lowest value 6.8301 D is observed for compound **3**. The average dipole moment decreases across the entitled compounds in the order **2** > **6** > **5** > **4** > **1** > **3**. To compare the values of dipole moment and first hyperpolarizability, the urea molecule is considered a standard molecule. All entitled molecules show a greater magnitude of dipole moment than the urea molecule which shows the value of 1.3732 D.[66] The dipole moment of all entitled compounds is found to be 5.42, 5.79, 4.97, 5.50, 5.57, and 5.57 D that is many times larger than that exhibited by the urea molecule. The average linear polarizability values for compounds (**1**−**6**) are observed to be 231.051, 230.391, 231.053, 241.695, 243.422, and 245.701 a.u, respectively. The greater total linear polarizability value 245.701 a.u is noticed in **6**, while **2** exhibits the lowest value 230.391 a.u of total linear polarizability. The order of $\boldsymbol{\alpha}_{tot}$ for examined compounds (**1**−**6**) is found to be in the following decreasing order: **6** > **5** > **4** > **3** > **1** > **2** (Table S15). In the case of first hyperpolarizability (β_{tot}), the values of nine contributing tensors β_{xxx}, β_{xyy}, β_{xyy}, β_{yyy}, β_{xxz}, β_{yyz}, β_{xzz}, β_{yzz}, and β_{zzz} along x-, y-, and z-directions and β_{tot} are tabulated in Table S16. The average β_{tot} values for compounds (**1**−**6**) are calculated to be 392.807, 501.709, 192.778, 408.93, 390.074, and 349.412 a.u, respectively. The highest and lowest values of β_{tot} between compounds (**1**−**6**) are examined to be 501.709 and 192.778 a.u in 2 and 3, respectively. The decreasing order of β_{tot} for the studied compounds (**1**−**6**) is **2** > **4** > **1** > **5** > **6** > **3**. The results are further compared with that of urea molecule [β_{tot} (urea) = 43 a.u][62] taken as standard to evaluate NLO behavior. Results revealed that β_{tot} values of compounds (**1**−**6**) are computed to be 9.13, 11.66, 4.48, 9.51, 9.07, and 8.12 a.u many times higher than that of the urea molecule. This urea-related inspection revealed that all investigated compounds were suitable to be NLO contestants.

https://doi.org/10.1021/acsomega.1c04984
ACS Omega 2021, 6, 33914−33922

4. CONCLUSIONS

A series of novel salicylaldehyde TSC compounds (**1**−**6**) are successfully synthesized and characterized by spectroscopic techniques. A comparative study of experimental and DFT calculated results is reported to reveal good agreement for vibrational and UV−vis assignments. NBO analysis revealed that all compounds are chemically stable due to different sorts of hyperconjugative interactions and ICT. The charge-transfer properties are determined quantitatively by FMO analysis. HOMO/LUMO energy gaps are explored in the span of 4.133−4.186 eV, and the energies associated with FMOs are utilized for the calculation of global reactivity descriptors which in turn signified the electron-donating ability and kinetic stability of newly synthesized molecules. Hyperpolarizability values of compounds (**1**−**6**) were observed as 9.13, 11.66, 4.48, 9.51, 9.07, and 8.12 a.u, respectively, that are many times greater as compared to that of the urea taken as the standard. These results represent the significant NLO character and may have a noteworthy role for technological applications. Hence, the studied compounds are recommended for further NLO studies to be utilized in modern technology.

5. EXPERIMENTAL SECTION

5.1. Synthesis of TSCs. Equimolar quantities of substituted thiosemicarbazide and 5-chloro salicylaldehyde were separately dissolved in ethanol. Both the solutions were mixed, and then, acetic acid was added. After mixing of solutions, the mixture was heated for 3 h till precipitation occurred, revealing the completion of the reaction according to Scheme 1. The solid mass of the ligand was filtered, then washed frequently by using ethanol, and dried. The extent of the reaction was observed via thin-layer chromatography during the reaction. The detailed synthetic scheme of TSCs was also discussed in our previously published article.[67]

5.2. (*E*)-*N*-Benzyl-2-(5-choro-2hydroxybenzyidene)-hydrazinecarbothioamide (1). Yield 85%; white crystalline: mp: 194 °C; IR (KBr), V (cm^{-1}): 1229 (C═S), 1548 (C═N), 3002, 3153 (NH) (Figure S8), UV−vis (ethanol): λ max 241 nm (Figure S2). ^{1}H NMR δ (ppm): 4.855 (d, J = 8.5 Hz, 2H, CH_2−NH), 9.094 (t, J = 8.5 Hz, 1H, NH−CH_2), 11.661 (s, 1H, NH−N), 10.277 (s, 1H, ═CH−N), 8.331 (s, OH−phenyl), 6.793−8.160 (m, 2 phenyl rings) (Figure S14).

5.3. (*E*)-2-(5-Chloro-2-hydroxybenzyidene)-*N*-(2-flurobenzyl)hyrazinecarbothioamide (2). Yield 82%; white crystalline: mp: 218 °C, IR (KBr), V (cm^{-1}): 1222 (C═S), 1532 (C═N), 3125, 3187 (NH) (Figure S9), UV−vis (ethanol): λ max 240 nm (Figure S3). ^{1}H NMR δ (ppm): 4.783 (d, J = 9 Hz, 2H, CH_2−NH), 9.138 (t, J = 8.5 Hz, 3H, NH−CH_2), 11.581 (s, 1H, NH−N), 10.264 (s, 1H, ═CH−N), 8.307 (s, 1H, OH−phenyl), 6.783−8.139 (m, 2 phenyl rings) (Figure S15).

5.4. 2-(5-Chloro-2-hydroxybenzylidene)-*N*-(4-flurobenzyl)hydrazinecarbothioamide (3). Yield 77%; white crystalline, mp: 202 °C, IR (KBr), V (cm^{-1}): 1217 (C═S), 1548 (C═N), 3187, 3125, (NH) (Figure S10), UV−vis (ethanol): λ max 220 nm (Figure S4). ^{1}H NMR δ (ppm): 4.787 (d, J = 7.5 Hz, 2H, CH_2−NH), 9.155 (t, J = 7.5 Hz, 1H, NH−CH_2), 11.601 (s, 1H, NH−N), 10.249 (s, 1H, N═CH), 8.320 (s, OH−phenyl), 6.839−8.050 (m, 2 phenyl rings) (Figure S16).

5.5. 2-(5-Chloro-2-hydroxybenzylidende)-*N*-(2-methylbenzyl) Hydrazinecarbothio Amide (4). Yield, 79%; white crystalline: mp: 220 °C; IR (KBr), V (cm^{-1}): 1228 (C═S), 1541 (C═N), 3134, 2996 (NH) (Figure S11), UV−vis (ethanol): λ max 219 nm (Figure S5). ^{1}H NMR δ (ppm): 2.257 (s, 3H, Ar−CH_3), 4.8415 (d, J = 7.5 Hz, 2H, CH_2−NH), 9.112 (d, J = 8.5 Hz, 1H, NH−CH_2), 11.663 (s, 1H, NH−N), 10.275 (s, 1H, N═CH), 8.323 (s, OH−phenyl), 6.831−8.051 (m, 2 phenyl rings) (Figure S17).

5.6. (*E*)-2-(5-Chloro-2-hydroxybenzylidene)-*N*-(3-methylbenzyl) Hydrazinecarbothio Amide (5). Yield, 82%; white crystalline: mp: 217 °C IR (KBr), V (cm^{-1}): 1223 (C═S), 1543 (C═N), 3218, 3125 (NH) (Figure S12), UV−vis (ethanol): λ max 296 nm (Figure S6). ^{1}H NMR, δ (ppm): 2.232 (s, 3H, Ar−CH_3) 4.751 (d, J = 8 Hz, 2H, CH_2−NH), 9.094 (s, 1H, NH−CH_2), 11.544 (s, 1H, NH−N), 10.236 (s, 6H, N═CH), 8.300 (s, OH−phenyl), 6.823−8.035 (m, 2 phenyl rings) (Figure S18).

5.7. (*E*)-2-(5-Chloro-2-hydroxybenzylidene)-*N*-(4-methylbenzyl)hydrazinecarbothio Amide (6). Yield, 79%; white crystalline: mp: 195 °C IR (KBr), V (cm^{-1}): 1225 (C═S), 1539 (C═N), 3094, 3130 (NH) (Figure S13), UV−vis (ethanol): λ max 245 nm (Figure S7). ^{1}H NMR δ (ppm): 2.257 (s, 3H, Ar−CH_3), 4.777 (d, J = 7.5 Hz, 2H, CH_2−NH), 9.127 (d, J = 8 Hz, 1H, NH−CH_2), 11.565 (s, 1H, NH−N), 10.242 (s, 1H, N═CH), 8.316 (s, OH−phenyl), 6.835−8.047 (m, 2 phenyl rings) (Figure S19).

■ ASSOCIATED CONTENT

Supporting Information

The Supporting Information is available free of charge at https://pubs.acs.org/doi/10.1021/acsomega.1c04984.

Computational details and UV−vis, IR, and NMR spectra (PDF)

■ AUTHOR INFORMATION

Corresponding Author

Muhammad Khalid − *Department of Chemistry, Khwaja Fareed University of Engineering & Information Technology, Rahim Yar Khan 64200, Pakistan;* orcid.org/0000-0002-1899-5689; Email: khalid@iq.usp.br, muhammad.khalid@kfueit.edu.pk

Authors

Muhammad Imran − *Department of Chemistry, Faculty of Science, King Khalid University, Abha 61413, Saudi Arabia*

Rifat Jawaria − *Department of Chemistry, Khwaja Fareed University of Engineering & Information Technology, Rahim Yar Khan 64200, Pakistan*

Asif Ali − *Department of Chemistry, Khwaja Fareed University of Engineering & Information Technology, Rahim Yar Khan 64200, Pakistan*

Muhammad Adnan Asghar − *Department of Chemistry, Division of Science and Technology, University of Education, Lahore 54770, Pakistan*

Zahid Shafiq − *Institute of Chemical Sciences, Bahauddin Zakariya University, Multan 60800, Pakistan;* orcid.org/0000-0003-4088-8297

Mohammed A. Assiri − *Department of Chemistry, Faculty of Science, King Khalid University, Abha 61413, Saudi Arabia*

Hafiza Munazza Lodhi − *Department of Chemistry, Khwaja Fareed University of Engineering & Information Technology, Rahim Yar Khan 64200, Pakistan*

https://doi.org/10.1021/acsomega.1c04984
ACS Omega 2021, 6, 33914−33922

Ataualpa Albert Carmo Braga − *Departamento de Química Fundamental, Instituto de Química, Universidade de São Paulo, São Paulo 05508-000, Brazil;* orcid.org/0000-0001-7392-3701

Complete contact information is available at: https://pubs.acs.org/10.1021/acsomega.1c04984

Notes

The authors declare no competing financial interest.

■ ACKNOWLEDGMENTS

M.I. and M.A.A. expresses appreciation to the Deanship of Scientific Research at the King Khalid University Saudi Arabia for funding through research groups program under grant number R.G.P. 2/153/42.

■ REFERENCES

(1) Hansen, T. V.; Skattebol, L. Ortho-Formylation of Phenols: Preparation of 3-Bromosalicylaldehyde:(3-Bromo-2-hydroxybenzaldehyde). *Org. Synth.* **2003**, *82*, 64−68.

(2) Mohan, C.; Kumar, V.; Kumari, N.; Kumari, S.; Yadav, J.; Gandass, T.; Yadav, S. Synthesis, Characterization and Antibacterial Activity of Semicarbazide Based Schiff Bases and their Pb (II), Zr (IV) and U (VI) Complexes. *J. Adv. Chem.* **2020**, *2*, 187−196.

(3) Miyamoto, K.; Koshiura, R.; Mori, M.; Yokoi, H.; Mori, C.; Hasegawa, T.; Takatori, K. Antitumor activity of 5-substituted 2-acylamino-1,3,4-thiadiazoles against transplantable rodent tumors. *Chem. Pharm. Bull.* **1985**, *33*, 5126−5129.

(4) Labanauskas, L.; Kalcas, V.; Udrenaite, E.; Gaidelis, P.; Brukstus, A.; Dauksas, V. Synthesis of 3-(3,4-dimethoxyphenyl)-1 H-1,2,4-triazole-5-thiol and 2-amino-5-(3,4-dimethoxyphenyl)-1,3,4-thiadiazole derivatives exhibiting anti-inflammatory activity. *Pharmazie* **2001**, *56*, 617−619.

(5) Turner, S.; Myers, M.; Gadie, B.; Hale, S. A.; Horsley, A.; Nelson, A. J.; Pape, R.; Saville, J. F.; Doxey, J. C.; Berridge, T. L. Antihypertensive thiadiazoles. 2. Vasodilator activity of some 2-aryl-5-guanidino-1,3,4-thiadiazoles. *J. Med. Chem.* **1988**, *31*, 906−913.

(6) Klayman, D. L.; Lin, A. J.; Hoch, J. M.; Scovill, J. P.; Lambros, C.; Dobek, A. S. 2-Acetylpyridine Thiosemicarbazones XI: 2-(α-Hydroxyacetyl)pyridine Thiosemicarbazones as Antimalarial and Antibacterial agents. *J. Pharm. Sci.* **1984**, *73*, 1763−1767.

(7) Liberta, A. E.; West, D. X. Antifungal and antitumor activity of heterocyclic thiosemicarbazones and their metal complexes: current status. *BioMetals* **1992**, *5*, 121−126.

(8) Klayman, D. L.; Scovill, J. P.; Bartosevich, J. F.; Bruce, J. 2-Acetylpyridine thiosemicarbazones. 5. 1-[1-(2-Pyridyl)ethyl]-3-thiosemicarbazides as potential antimalarial agents. *J. Med. Chem.* **1983**, *26*, 35−39.

(9) Sharma, S.; Athar, F.; Maurya, M. R.; Azam, A. Copper(II) complexes with substituted thiosemicarbazones of thiophene-2-carboxaldehyde: synthesis, characterization and antiamoebic activity against E. histolytica. *Eur. J. Med. Chem.* **2005**, *40*, 1414−1419.

(10) Lobana, T. S.; Rekha; Butcher, R. J.; Castineiras, A.; Bermejo, E.; Bharatam, P. V. Bonding Trends of Thiosemicarbazones in Mononuclear and Dinuclear Copper(I) Complexes: Syntheses, Structures, and Theoretical Aspects. *Inorg. Chem.* **2006**, *45*, 1535−1542.

(11) Shahlaei, M.; Fassihi, A.; Nezami, A. Qsar study of some 5-methyl/trifluoromethoxy-1H-indole-2,3-dione-3-thiosemicarbazone derivatives as anti-tubercular agents. *Results Pharma Sci.* **2009**, *4*, 123.

(12) Pahontu, E.; Julea, F.; Rosu, T.; Purcarea, V.; Chumakov, Y.; Petrenco, P.; Gulea, A. Antibacterial, antifungal and in vitro antileukaemia activity of metal complexes with thiosemicarbazones. *J. Cell. Mol. Med.* **2015**, *19*, 865−878.

(13) Pagano, M.; Demoro, B.; Toloza, J.; Boiani, L.; González, M.; Cerecetto, H.; Olea-Azar, C.; Norambuena, E.; Gambino, D.; Otero, L. Effect of ruthenium complexation on trypanocidal activity of 5-nitrofuryl containing thiosemicarbazones. *Eur. J. Med. Chem.* **2009**, *44*, 4937−4943.

(14) Chapleo, C. B.; Myers, P. L.; Smith, A. C. B.; Stillings, M. R.; Tulloch, I. F.; Walter, D. S. Substituted 1,3,4-thiadiazoles with anticonvulsant activity. 4. Amidines. *J. Med. Chem.* **1988**, *31*, 7−11.

(15) Struga, M.; Kossakowski, J.; Kedzierska, E.; Fidecka, S.; Stefan, J. Synthesis and Pharmacological Activity of Urea and Thiourea Derivatives of 4-Azatricyclo[5.2.2.02,6]undec-8-ene-3,5-dione. *Chem. Pharm. Bull.* **2007**, *55*, 796−799.

(16) Mazzone, G.; Pignatello, R.; Mazzone, S.; Panico, A.; Pennisi, G.; Castana, R.; Mazzone, P. Synthesis and local anesthetic activity of alkylaminoacyl derivatives of 2-amino-1,3,4-thiadiazole. *Farmaco* **1993**, *48*, 1207−1224.

(17) Hanna, M. A.; Girges, M. M.; Rasala, D.; Gawinecki, R. Synthesis and pharmacological evaluation of some novel 5-(pyrazol-3-yl)thiadiazole and oxadiazole derivatives as potential hypoglycemic agents. *Arzneimittelforschung* **1995**, *45*, 1074−1078.

(18) Andreani, A.; Granaiola, M.; Leoni, A.; Locatelli, A.; Morigi, R.; Rambaldi, M. Synthesis and antitubercular activity of imidazo[2,1-b]thiazoles. *Eur. J. Med. Chem.* **2001**, *36*, 743−746.

(19) Holla, B. S.; Malini, K. V.; Rao, B. S.; Sarojini, B. K.; Kumari, N. S. Synthesis of some new 2,4-disubstituted thiazoles as possible antibacterial and anti-inflammatory agents. *Eur. J. Med. Chem.* **2003**, *38*, 313−318.

(20) Padhyé, S.; Kauffman, G. B. Transition metal complexes of semicarbazones and thiosemicarbazones. *Coord. Chem. Rev.* **1985**, *63*, 127−160.

(21) Güveli, Ş.; Koca, A.; Ozdemir, N.; Bal-Demirci, T.; Ülküseven, B. Electrochemistry and structural properties of new mixed ligand nickel (II) complexes based on thiosemicarbazone. *New J. Chem.* **2014**, *38*, 5582−5589.

(22) Prasad, S.; Agarwal, R. K. Cobalt(II) complexes of various thiosemicarbazones of 4-aminoantipyrine: syntheses, spectral, thermal and antimicrobial studies. *Transition Met. Chem.* **2007**, *32*, 143−149.

(23) Silva-Junior, M. R.; Schreiber, M.; Sauer, S. P. A.; Thiel, W. Benchmarks for electronically excited states: Time-dependent density functional theory and density functional theory based multireference configuration interaction. *J. Chem. Phys.* **2008**, *129*, 104103.

(24) Mahmood, A.; Akram, T.; de Lima, E. B. Syntheses, spectroscopic investigation and electronic properties of two sulfonamide derivatives: a combined experimental and quantum chemical approach. *J. Mol. Struct.* **2016**, *1108*, 496−507.

(25) Ghiasuddin; Akram, M.; Adeel, M.; Khalid, M.; Tahir, M. N.; Khan, M. U.; Asghar, M. A.; Iqbal, M. A combined experimental and computational study of 3-bromo-5-(2, 5-difluorophenyl) pyridine and 3, 5-bis (naphthalen-1-yl) pyridine: Insight into the synthesis, spectroscopic, single crystal XRD, electronic, nonlinear optical and biological properties. *J. Mol. Struct.* **2018**, *1160*, 129−141.

(26) Marder, S. R.; Sohn, J. E.; Stucky, G. D. *Materials for nonlinear optics chemical perspectives*; Am Chem Soc: Washington DC, 1991.

(27) Shahid, M.; Salim, M.; Khalid, M.; Tahir, M. N.; Khan, M. U.; Braga, A. A. C. Synthetic, XRD, non-covalent interactions and solvent dependent nonlinear optical studies of Sulfadiazine-Ortho-Vanillin Schiff base: (E)-4-((2-hydroxy-3-methoxy- benzylidene) amino)-N-(pyrimidin-2-yl)benzene-sulfonamide. *J. Mol. Struct.* **2018**, *1161*, 66−75.

(28) Ahmad, M. S.; Khalid, M.; Shaheen, M. A.; Tahir, M. N.; Khan, M. U.; Braga, A. A. C.; Shad, H. A. Synthesis and XRD, FT-IR vibrational, UV-vis, and nonlinear optical exploration of novel tetra substituted imidazole derivatives: A synergistic experimental-computational analysis. *J. Phys. Chem. Solids* **2018**, *115*, 265−276.

(29) Khalid, M.; Ali, A.; Jawaria, R.; Asghar, M. A.; Asim, S.; Khan, M. U.; Hussain, R.; Fayyaz ur Rehman, M.; Ennis, C. J.; Akram, M. S. First principles study of electronic and nonlinear optical properties of A-D-π-A and D-A-D-π-A configured compounds containing novel quinoline-carbazole derivatives. *RSC Adv.* **2020**, *10*, 22273−22283.

(30) Zhao, Y.; Truhlar, D. G. The M06 suite of density functionals for main group thermochemistry, thermochemical kinetics, noncovalent interactions, excited states, and transition elements: two new

functionals and systematic testing of four M06-class functionals and 12 other functionals. *Theor. Chem. Acc.* **2008**, *120*, 215−241.
(31) Poirier, R.; Kari, R.; Csizmadia, I. G. *Handbook of Gaussian basis sets*; Elsevier, 1985.
(32) Mackenzie, C. F.; Spackman, P. R.; Jayatilaka, D.; Spackman, M. A. CrystalExplorermodel energies and energy frameworks: extension to metal coordination compounds, organic salts, solvates and open-shell systems. *IUCrJ* **2017**, *4*, 575−587.
(33) Ali, A.; Khalid, M.; Din, Z. U.; Asif, H. M.; Imran, M.; Tahir, M. N.; Ashfaq, M.; Rodrigues-Filho, E. Exploration of structural, electronic and third order nonlinear optical properties of crystalline chalcone systems: Monoarylidene and unsymmetrical diarylidene cycloalkanones. *J. Mol. Struct.* **2021**, *1241*, 130685.
(34) Bader, R. F. W. Bond paths are not chemical bonds. *J. Phys. Chem. A* **2009**, *113*, 10391−10396.
(35) Rasool, F.; Khalid, M.; Yar, M.; Ayub, K.; Tariq, M.; Hussain, A.; Lateef, M.; Kashif, M.; Iqbal, S. Facile synthesis, DNA binding, Urease inhibition, anti-oxidant, molecular docking and DFT studies of 3-(3-Bromo-phenyl)-1-(2-trifluoromethyl-phenyl)-propenone and 3-(3-Bromo-5 chloro-phenyl)-1-(2-trifluoromethyl-phenyl)-propenone. *J. Mol. Liq.* **2021**, *336*, 116302.
(36) Gross, E. K. U.; Kohn, W. Time-Dependent Density-Functional Theory. *Density Functional Theory of Many-Fermion Systems*; Elsevier, 1990; vol. *21*; pp 255−291.
(37) Burke, K.; Werschnik, J.; Gross, E. K. U. Time-dependent density functional theory: Past, present, and future. *J. Chem. Phys.* **2005**, *123*, 062206.
(38) Khan, I.; Khalid, M.; Adeel, M.; Niaz, S. I.; Shafiq, I.; Muhammad, S.; Braga, A. A. C. Palladium-catalyzed synthesis of 5-(arylated) pyrimidines, their characterization, electronic communication, and non-linear optical evaluations. *J. Mol. Struct.* **2021**, *1237*, 130408.
(39) Majumdar, D.; Das, D.; Nag, S.; Bhattacharyya, M.; Singh, D. K.; Parai, D.; Bankura, K.; Mishra, D. A rare hetero-bimetallic Zn(II)/Ca(II) Schiff base complex: Synthesis, crystal structure, DFT, molecular docking and unveiling antimicrobial activity. *J. Mol. Struct.* **2020**, *1222*, 128951.
(40) Park, Y.-S.; Park, J.-S.; Lee, S.; Jung, S.-H.; Kim, S.-K.; Ryu, C.-M. Simultaneous profiling of Arabidopsis thaliana and Vibrio vulnificus MO6-24/O transcriptomes by dual RNA-seq analysis. *Comput. Struct. Biotechnol. J.* **2021**, *19*, 2084−2096.
(41) Rafiq, M.; Khalid, M.; Tahir, M. N.; Ahmad, M. U.; Khan, M. U.; Naseer, M. M.; Shafiq, Z. Synthesis, XRD, spectral (IR, UV−Vis, NMR) characterization and quantum chemical exploration of benzoimidazole-based hydrazones: A synergistic experimental-computational analysis. *Appl. Organomet. Chem.* **2019**, *33*, No. e5182.
(42) Adeel, M.; Braga, A. A. C.; Tahir, M. N.; Haq, F.; Khalid, M.; Halim, M. A. Synthesis, X-ray crystallographic, spectroscopic and computational studies of aminothiazole derivatives. *J. Mol. Struct.* **2017**, *1131*, 136−148.
(43) Reed, A. E.; Weinhold, F.; Weiss, R.; Macheleid, J. Nature of the contact ion pair trichloromethyl-chloride (CCl3+Cl-). A theoretical study. *J. Phys. Chem. A* **1985**, *89*, 2688−2694.
(44) Glendening, E. D.; Landis, C. R.; Weinhold, F. 6 Natural bond orbital theory: Discovering chemistry with NBO7. *Complementary Bonding Analysis*; De Gruyter, 2021; pp 129−156.
(45) Khalid, M.; Ali, M.; Aslam, M.; Sumrra, S. H.; Khan, M. U.; Raza, N.; Imran, M. Frontier molecular, Natural bond orbital, UV-Vis spectral stduy, Solvent influence on geometric parameters, Vibrational frequencies and solvation energies of 8-Hydroxyquinoline. *Int. J. Pharma Sci. Res.* **2017**, *8*, 13040.
(46) Scott, A. P.; Radom, L. Harmonic Vibrational Frequencies: An Evaluation of Hartree−Fock, Møller−Plesset, Quadratic Configuration Interaction, Density Functional Theory, and Semiempirical Scale Factors. *J. Phys. Chem.* **1996**, *100*, 16502−16513.
(47) Socrates, G. *Infrared and Raman Characteristic Group Frequencies*; John Wiley & Sons Ltd: England, 2001.
(48) Silverstein, R. M.; Bassler, G. C.; Morril, T. C. *Spectroscopic Identification of Organic Compounds 4*; John Wiley and Sons Inc.: New York, 1981.
(49) Sathiyanarayanan, D. N. *Vibrational spectroscopy theory and application*; New Age International Publishers: New Delhi, 2004; p 424.
(50) Teimouri, A.; Chermahini, A. N.; Taban, K.; Dabbagh, H. A. Experimental and CIS, TD-DFT, ab initio calculations of visible spectra and the vibrational frequencies of sulfonyl azide-azoic dyes. *Spectrochim. Acta, Part A* **2009**, *72*, 369−377.
(51) Balachandran, V.; Lakshmi, A.; Janaki, A. Vibrational spectroscopic studies and Natural Bond Orbital analysis of 4,6-dichloro-2-(methylthio)pyrimidine based on density functional theory. *Spectrochim. Acta, Part A* **2011**, *81*, 1−7.
(52) Khan, M. U.; Iqbal, J.; Khalid, M.; Hussain, R.; Braga, A. A. C.; Hussain, M.; Muhammad, S. Designing triazatruxene-based donor materials with promising photovoltaic parameters for organic solar cells. *RSC Adv.* **2019**, *9*, 26402−26418.
(53) Srnec, M.; Solomon, E. I. Frontier molecular orbital contributions to chlorination versus hydroxylation selectivity in the non-heme iron halogenase SyrB2. *J. Am. Chem. Soc.* **2017**, *139*, 2396−2407.
(54) Kandemirli, F.; Sagdinc, S. Theoretical study of corrosion inhibition of amides and thiosemicarbazones. *Corros. Sci.* **2007**, *49*, 2118−2130.
(55) Amiri, S. S.; Makarem, S.; Ahmar, H.; Ashenagar, S. Theoretical studies and spectroscopic characterization of novel 4-methyl-5-((5-phenyl-1,3,4-oxadiazol-2-yl)thio)benzene-1,2-diol. *J. Mol. Struct.* **2016**, *1119*, 18−24.
(56) Ali, A.; Khalid, M.; Abid, S.; Iqbal, J.; Tahir, M. N.; Rauf Raza, A.; Paixao, M. W. Facile synthesis, crystal growth, characterization and computational study of new pyridine-based halogenated hydrazones: Unveiling the stabilization behavior in terms of noncovalent interactions. *Appl. Organomet. Chem.* **2020**, *34*, No. e5399.
(57) Parr, R. G.; Szentpály, L. V.; Liu, S. Electrophilicity index. *J. Am. Chem. Soc.* **1999**, *121*, 1922−1924.
(58) Parr, R. G.; Donnelly, R. A.; Levy, M.; Palke, W. E. Electronegativity: the density functional viewpoint. *J. Chem. Phys.* **1978**, *68*, 3801−3807.
(59) Parr, R. G.; Szentpály, L. V.; Liu, S. Electrophilicity index. *J. Am. Chem. Soc.* **1999**, *121*, 1922−1924.
(60) Gao, L.; Huang, J.; Guo, S.; Yang, Z.; Pan, S. Structure-property survey and computer-assisted screening of mid-infrared nonlinear optical chalcohalides. *Coord. Chem. Rev.* **2020**, *421*, 213379.
(61) Ivonina, M. V.; Orimoto, Y.; Aoki, Y. Nonlinear optical properties of push-pull systems containing [2.2]paracyclophane: Theoretical study via elongation method. *Chem. Phys. Lett.* **2020**, *755*, 137760.
(62) Yao, Y.; Zhang, Y.; Li, X.; Qiu, Y.-Q. The second-order NLO property of a photoswitchable heteroditpioc ion-pair receptor based on 2-pyridyl acylhydrazone linking with 2,6-pyridine bisamide: The impacts of metal cations and anions. *J. Mol. Graphics Modell.* **2020**, *100*, 107652.
(63) Gauthier, S.; Porter, A.; Achelle, S.; Roisnel, T.; Dorcet, V.; Barsella, A.; Le Poul, N.; Guevara Level, P.; Jacquemin, D.; Robin-Le Guen, F. Mono- and Diplatinum Polyynediyl Complexes as Potential Push-Pull Chromophores: Synthesis, Characterization, TD-DFT Modeling, and Photophysical and NLO Properties. *Organometallics* **2018**, *37*, 2232−2244.
(64) Ullah, F.; Kosar, N.; Ayub, K.; Gilani, M. A.; Mahmood, T. Theoretical study on a boron phosphide nanocage doped with superalkalis: novel electrides having significant nonlinear optical response. *New J. Chem.* **2019**, *43*, 5727−5736.
(65) Karakas, A.; Elmali, A.; Unver, H. Linear optical transmission measurements and computational study of linear polarizabilities, first hyperpolarizabilities of a dinuclear iron(III) complex. *Spectrochim. Acta, Part A* **2007**, *68*, 567−572.
(66) Prasad, P. N.; Williams, D. J. *Introduction to nonlinear optical effects in molecules and polymers*; Wiley: New York, 1991; p 1.

https://doi.org/10.1021/acsomega.1c04984
ACS Omega 2021, 6, 33914−33922

(67) Khalid, M.; Jawaria, R.; Khan, M. U.; Braga, A. A. C.; Shafiq, Z.; Imran, M.; Irfan, A. An Efficient Synthesis, Spectroscopic Characterization, and Optical Nonlinearity Response of Novel Salicylaldehyde Thiosemicarbazone Derivatives. *ACS Omega* **2021**, *6* (24), 16058−16065.

https://doi.org/10.1021/acsomega.1c04984
ACS Omega 2021, 6, 33914−33922